Received: 23 December 2016 | Revised: 5 March 2017 | Accepted: 5 March 2017

DOI: 10.1002/aoc.3829

FULL PAPER

WILEY Applied Organometallic Chemistry

Novel structures of Zn(II) biometal cation with the biologically active substituted acetic acid and nitrogen donor ligands: Synthesis, spectral, phosphate diester catalytic hydrolysis and anti-microbial studies

Hijazi Abu Ali[†] | **Shayma Kamel**[†] | **Amani Abu Shamma**

Department of Chemistry, Birzeit University, West Bank, Palestine

Correspondence
Hijazi Abu Ali, Department of Chemistry, Birzeit University, P.O. Box 14, West Bank, Palestine.
Email: habuali@birzeit.edu; habuali1@yahoo.com

The complexes [Zn(methoxyacetate)$_2$1,10-phenanthroline] **1** and [Zn_2(phenylacetate)$_4$(quinoline)$_2$] **2**, were prepared and characterized by IR-spectroscopy, UV–Visible spectroscopy, ^{1}H and ^{13}C NMR spectroscopy, single crystal X-ray diffraction. BNPP hydrolysis of the complexes and their parent nitrogen ligands were scanned, the results indicated that the hydrolysis rates of BNPP were 4.5×10^4 and 6.2×10^5 for (**1**) and (**2**), respectively. In addition, anti-bacterial activities were scanned to investigate the effect of complexation on their activity against Gram-positive (*S. epidermidis*, *S. aureus*, *E. faecalis*, *M. luteus* and *B. Subtilis*) and Gram-negative (*K. pneumonia*, *E. coli*, *P. Mirabilis* and *P. Aeruginosa*) bacteria using agar well-diffusion method. Complex **1** showed high activity against $G^-$and G^+ bacteria except against *E. faecalis* and *P. Aeruginosa*. Complex **2** did not show any activity against G^- or G^+ bacteria.

KEYWORDS
anti-bacterial activity, hydrolysis, methoxyacetate, nitrogen donor ligands, phenylacetate, zinc(II) complexes

1 | INTRODUCTION

As natural constituents or substances introduced into the human body, biometal cations interact easily with molecules of water and various parts of different organic and inorganic biomolecules in biological systems forming various complexes., The complexes which associate via O-, N- and S- donor atoms, have important roles in biological processes. The products of interaction between M(II) metals and medicine are fundamentally important for the theory of coordination chemistry and significant in the development of new methods for determining micro-amounts of active components.[1–4] The study of the interaction between M(II) biometal–O-donor ligands is interesting for a variety of aspects including achievement of better balanced medicine dosage, improved anti-ulcerous, anti-tumor and anti-bacterial activity, and biodistribution of medicine while monitoring its pharmacokinetics, excretion; the reduction in the unwanted responses, improving anti-microbial activities and synergistic effects of the metals and medicine, and [1,5–12].

Biometals from the series of d-metals with characteristic M(II) ions can be found in the human body in small amounts, and are mainly the active centers of enzymes of various functions.[1,13]

Metals such as iron (Fe), zinc (Zn), and copper (Cu) all play important roles in many of the enzymatic reactions.[14]

Zinc is a biometal necessary for the growth and development of mammals, and in the human body, approximately 2 to 3 g of this metal can be found in the structure of more than twenty metalloenzymes (carbohydrase, alcohol dehydrogenase, Cu-Zn superoxide dismutase, etc). Zinc ion along with the Cu(II) and Co(II) ions improves the immune system of

[†]Author contributions: These authors have contributed equally to this work

humans.[15] Many biological processes require transition metals such as cell division which requires (Fe, Co), respiration requires (Fe, Cu), nitrogen fixation which requires (Fe, Mo, V), and photosynthesis which requires (Mn, Fe).[16]

In this work, phenylacetic acid and methoxyacetic acid, Figure 1, were selected to synthesize the complexes which were characterized using different technique. Phenylacetic acid belongs to an important class of compounds that is used in several industrial applications, such as flavors and fragrances in cosmetics or food. It also plays an important role in pharmaceutical industry as precursors or drugs. For example, phenylacetic acid can act as a precursor for analgesics like diclofenac. Moreover, penicillin-based antibiotics can be synthesized from phenylacetic acid.[17]

The second carboxylic acid is methoxyacetic acid, a primary metabolite of phthalates ester that is used in many manufacturing products. It was also reported that methoxyacetic acid has anti-cancer activities, especially prostate cancer. Researchers have found that methoxyacetic acid can induce apoptosis and inhibits the growth of prostate cancer cells.[18,19]

Metals can have many catalytic activity applications such as the hydrolysis of phosphate esters, and also in the detoxification of man-made phosphorous(V) toxin of some chemical weapons and pesticides. Actually the hydrolysis of these phosphate esters is very important in chemistry, biochemistry, and the mechanism of phosphodiester bond hydrolysis, both non-enzymatic and enzymatic, have been highly important for physical organic chemists.[20]

Different studies showed that the spontaneous reaction for the hydrolysis of a phosphodiesters bond under physiological conditions is first order with rate constant (k) which has been approximated to be $1*10^{-11}$ s^{-1} and $1*10^{-10}$ s^{-1} for double strand and single strand DNA, respectively.[21]

These rates can be improved by changing the pH, the concentration of metal ions and controlling the temperature at 37°C on a physiologically relevant time scale. 'bis(p-nitrophenyl)phosphate' (BNPP) shown in Figure 2 is a distinctive example of phosphate esters,[22] rapid hydrolysis of the high stable phosphate diester bond in *bis*-(*p*-nitrophenyl) phosphate (BNPP) by enzymes or catalysts containing metal ion complexes have recently been achieved.[23,24]

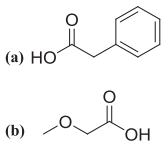

FIGURE 1 Carboxylic acids used in the present work: **A)** Phenylacetic acid, **B)** Methoxyacetic acid

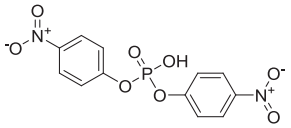

FIGURE 2 BNPP ($C_{12}H_9N_2O_8P$)

2 | EXPERIMENTAL

2.1 | Chemicals, materials and biological species

All reagents, chemicals and solvents used in the present work were purchased from Sigma-Aldrich with high purity and were used without further purification.

2.2 | Physical measurements

Solid samples with anhydrous potassium bromide (KBr) were ground and compressed into a disc to use them for IR spectral measurements which were recorded in the 200–4000 cm^{-1} region using TENSOR II FT-IR Spectrometer (BRUKER). UV–Vis spectra were recorded using an Agilent 8453 photodiode array (PDA) spectrophotometer in the 200–600 nm region using CH_3OH as a solvent. NMR spectra were recorded using a Varian Unity Spectrometer operating at 300 MHz for ^1H and ^{13}C nucleus. Melting points were determined using capillary tubes with Electrothermal apparatus, and X-ray analyses were performed using SMART APEX CCD X-ray diffractometer (Bruker).

2.3 | Synthesis and characterization of zinc(II) compounds

All zinc(II) compounds were prepared at room temperature.

2.3.1 | Zinc methoxyacetate1,10-phenanthroline [Zn(methoxy)$_2$1,10-phen] (1)

In (1:1) ratio sodium hydroxide (4.9 mmol, 0.20 g), and methoxyacetic acid (0.32 g) in 50 ml of MeOH were mixed and dissolved. Then (3.5 mmol, 0.48 g) $ZnCl_2$ in minimum amount of MeOH was added and the reaction mixture was stirred for an additional 12 h. The solid product was filtered and washed with cold water and air dried to give 1 g of solid product. The prepared Zn-methoxy (2.6 mmol, 0.41 g) was dissolved in 50 ml MeOH and 1,10-phenanthroline (2.6 mmol, 0.41 g) dissolved in a minimum amount of MeOH was added to the stirred Zn-methoxy solution. Immediately a white precipitate was formed and the reaction mixture was stirred for an additional 24 h. The solution was filtered, the filtrate was then allowed to evaporate slowly and solid crystals were obtained. Recrystallization from MeOH gave single crystals suitable for X-ray analysis.

[Zn(methoxy)$_2$1,10-phen] (1)

90% yield; m.p. 190–196°C; ^{1}H NMR ($CDCl_3$): δ (ppm) 3.50 (s, 3H, CH_3), 4.03 (s, 2H, CH_2),7.83 (m, 2H, CH), 7.94 (s, 2H, CH), 8.46 (d, 2H, CH, $^3J_{H\text{-}H}$ = 7.8 Hz), 9.18 (dd, 2H, CH, $^3J_{H\text{-}H}$ = 6.3 Hz);^{13}C{^{1}H}-NMR ($CDCl_3$): δ (ppm) 59.01 (CH_3), 71.21 (CH_2), 124.25 (CH), 124.29 (CH), 126.79 (CH), 128.80 (CH), 149.97 (CH), 150.01(CH) 173.84 (C = O); IR (cm^{-1}, KBr): 3046, 2995, 1597.1, 1514.22, 1425.9, 1342, 1101, 849.01, 726.37; UV–Vis (MeOH, λ (nm)): 271, 292.

2.3.2 | Zinc phenylacetate complex

Sodium hydroxide (1.0 mmol, 1.5 g), and phenylacetic acid (1.0 mmol, 5.0 g) were mixed in 100 ml of MeOH and stirred for 3 h. Then the solvent was evaporated to give a needle solid which was re-dissolved in MeOH, and $ZnCl_2$ (1.0 mmol, 5.0 g) dissolved in 15 ml of MeOH was added with stirring. The reaction mixture was stirred for additional 12 h; the white precipitate of Zinc phenylacetate was then filtered, washed with cold water and air dried to give 4.4 g of solid product. Percentage yield was 89%; m.p. > 200°C; ^{1}H NMR ($CDCl_3$): δ (ppm) 3.39 (s, 2H, CH_2), 7.21 (s, 5H, CH); ^{13}C{^{1}H}-NMR ($CDCl_3$): δ (ppm) 43.11 (CH_2), 126.21 (CH), 128.31 (CH), 129.69 (CH), 137.91 (C), 176.98 (C = O); IR(cm^{-1}, KBr): 3444, 2350, 1531, 1439, 1391, 723; UV–Vis (MeOH, λ (nm)): 214, 259, 265.

2.3.3 | Zinc phenylacetatequinolinecomplex [Zn$_2$(phenyl)$_4$(quin)$_2$] (2)

Zn-phenyl (2.0 mmol, 0.40 g) was dissolved in 50 ml MeOH (insoluble) and quinoline (4.0 mmol, 0.52 g) dissolved in minimum amount of MeOH was added to the Zn-phenyl solution with stirring. The reaction mixture was stirred for 12 h. Dichloromethane was then added until the solution became clear, and the solution was allowed to evaporate slowly to give solid crystals suitable for X-ray analysis.

[Zn$_2$(phenyl)$_4$(quin)$_2$] (2)

Percentage yield was 87%; m.p. = 144°C; ^{1}H NMR (DMSO): δ (ppm) 3.39 (s, 2H, CH_2), 7.22 (bs, 5H, CH), 7.56 (m, 2H, CH), 7.75 (m, 1H, CH), 7.98 (m, 2H, CH), 8.35 (d, 1H, CH, $^3J_{H\text{-}H}$ = 8.1 Hz), 8.88 (bs, 1H, CH); ^{13}C{^{1}H}-NMR ($CDCl_3$): δ (ppm) 43.99 (CH_2), 122.68 (CH), 126.97 (CH), 127.81 (CH), 129.10 (C), 129.32 (C), 129.99 (CH), 130.48 (CH), 130.80 (CH), 137.47 (C), 138.74 (CH), 151.82 (CH), 177.64 (C = O); IR (cm^{-1}, KBr): 3027, 2362, 1946, 1588, 1403, 1316, 809; UV–Vis (MeOH, λ (nm)): 276, 287.

2.4 | X-ray crystallography

Single crystal X-ray analysis of complexes **1** and **2** were carried out by attaching single crystal to a glass fiber with epoxy glue, and then it was transferred to X-ray diffractometer system (Bruker SMART APEX CCD) which was controlled by a Pentium-based PC equipped with SMART software package.[25] The diffracted graphite-monochromated (Kα radiation λ = 0.71073 Å) was detected on a phosphor screen at -44°C and it was held at 6.0 cm from the crystal. A detector array of 512 X 512 pixels (a pixel size ≈120 μm) was used to collect the data.[26] Results of X-ray crystallography and structure refinements are shown in Table 1.

2.5 | Kinetic measurements of BNPP hydrolysis

Optimal concentrations and conditions for the BNPP hydrolysis were chosen by running different UV–visible kinetic experiments and the best absorbance versus time plots were used to determine the optimal conditions.

The following conditions were used for all hydrolysis reactions:

HEPES'4-(2-hydroxyethyl)-1-piperazineethanesulfonic acid') buffer at concentration of 50 μM was prepared by dissolving the appropriate amount of HEPES in minimum amount of deionized water, then adjusting the pH to 7.91 using HCl or NaOH and the final volume was completed to 100 ml. (0.036 g) of BNPP was dissolved in the prepared buffer to obtain a certain concentration of 1.0x10^{-3} M. The desired complex concentration was prepared in methanol, the two solutions were kept in a water bath at 25°C for 10 minutes, then (1.5 ml) of the two solutions were mixed in a quartz cell at 25°C, the rate of release of p-nitrophenol was directly measured using UV–Vis spectrophotometer at λ = 400 nm and an extinction coefficient of 13400 Lmol^{-1} cm^{-1}. The effect of BNPP concentration on the hydrolysis process was studied by measuring the rate of hydrolysis at 10^{-4} and 10^{-5} M.[27]

3 | RESULTS AND DISCUSSION

3.1 | Synthesis of Zn(II) complexes

One equivalent of $ZnCl_2$ was reacted with 1 equivalent of sodium methoxyacetate and sodium phenylacetate in methanol to give [Zn(methoxy)$_2$(H_2O)$_2$] and [Zn(phen)$_2$(H_2O)$_2$], respectively, as shown in Scheme 1. (Table 2)

Different nitrogen donor ligands were mixed with the synthesized zinc methoxy and zinc phenyl acetate and their structures are shown in Schemes 2 and 3 respectively. The proposed structures are also supported by their single crustal X-ray structure analysis.

TABLE 1 Structure refinement and results of X-ray crystallography of compounds (**1**) and (**2**)

	Complex (1)	Complex (2)
Empirical formula	$C_{18}H_{22}N_2O_8Zn$	$C_{50}H_{42}N_2O_8Zn_2$
Formula weight	459.75	929.60
Temperature	295(2) K	296(1) K
Wavelength	0.71073 Å	0.71073 Å
Crystal system	Monoclinic	Triclinic
Space group	C2/c	P-1
Unit cell dimensions	a = 14.287(2) Å α = 90°. b = 10.137(1) Å β = 104.011(2)°. c = 28.861(4) Å γ = 90°.	a = 8.464(2) Å α = 95.179(3)°. b = 11.165(2) Å β = 108.293(3). c = 12.160(3) Å γ = 93.175(3)°.
Volume	4055.2(9) $Å^3$	1082.4(4) $Å^3$
Z	8	1
Density (calculated)	1.506 Mg/m^3	1.426 Mg/m^3
Absorption coefficient	1.259 mm^{-1}	1.166 mm^{-1}
F(000)	1904	480
Crystal size	0.40 x 0.29 x 0.14 mm^3	0.52 x 0.51 x 0.40 mm^3
Theta range for data collection	2.49 to 28.03°.	2.41 to 26.00°.
Index ranges	−18 < =h < =18,-13 < =k < =13, −38 < =l < =37	−10 < =h < =10,-13 < =k < =13, −14 < =l < =14
Reflections collected	22840	10335
Independent reflections	4880 [R(int) = 0.0268]	4095 [R(int) = 0.0323]
Completeness to theta =28.03°	98.9%	96.1%
Absorption correction	Semi-empirical from equivalents	Semi-empirical from equivalents
Max. and min. transmission	0.8435 and 0.6329	0.6527 and 0.5823
Data / restraints / parameters	4880 / 0 / 264	4095 / 0 / 280
Goodness-of-fit on F^2	1.199	1.140
Final R indices [$I > 2$sigma(I)]	R1 = 0.0508, wR2 = 0.116	R1 = 0.0546, wR2 = 0.1662
R indices (all data)	R1 = 0.0562, wR2 = 0.1191	R1 = 0.0583, wR2 = 0.1675
Largest diff. peak and hole	0.478 and −0.400 e.$Å^{-3}$	1.274 and −0.362 e.$Å^{-3}$

a $R1 = \sum||Fo| - |Fc|| / \sum|Fo|$ and $wR2 = \sum[w(F02 - Fc2)2]/\sum[w(Fo2)2]$ 1/2

TABLE 2 Physical properties and yield of zinc(II) complexes

Complex	%Yield	m.p (°C)	Solubility
1	90	190–196	Hot CH_3OH, DMSO
2	87	144	DMSO,CH_2Cl_2

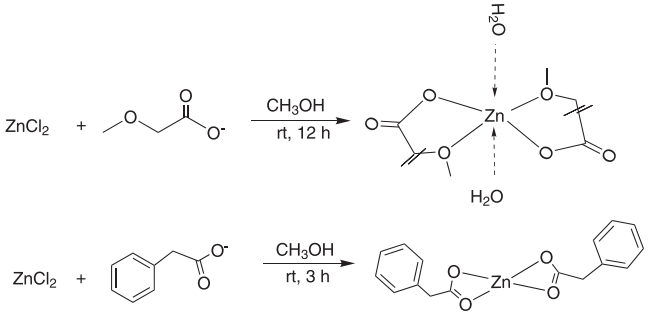

SCHEME 1 Synthesis and proposed structure of zinc(II) complexes

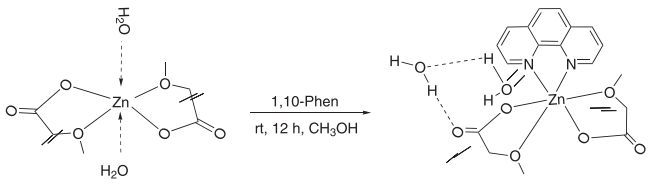

SCHEME 2 Synthesis and proposed structure of zinc(II) complex **1**

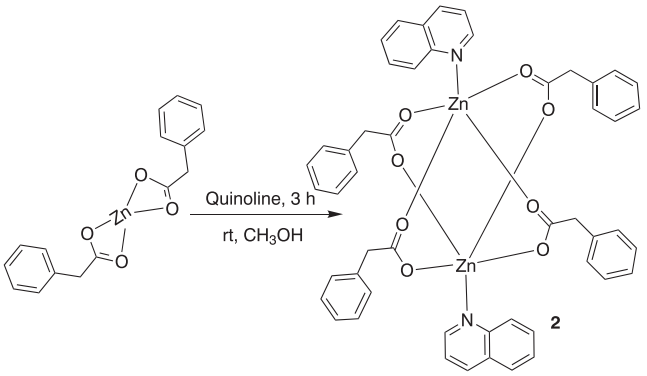

SCHEME 3 Synthesis and proposed structure of zinc(II) complex **2**

3.2 | Crystallographic study

3.2.1 | X-ray crystal structure of [Zn(methoxy)$_2$1,10-phen] (1)

Figure 3 shows the crystal structure of complex **1** with two bidentate methoxyacetate groups and one bidentate 1,10-phenligand, both ligands formed stable five member ring with Zn as the metal center.

Further stability of the crystal lattice was achieved by the intramolecular hydrogen bonding between the two water molecules and the carbonyl oxygen atom of one methoxyacetate groups as illustrated by the dashed lines which occur within one single molecule.[28] In addition, both intramolecular and intermolecular hydrogen bonding play a crucial role in the enhancement of complex stability, for example, H-bonds give conformational stability of protein and other complex structures such as [29,30]. The bond distances of O-Zn (2.0269(19) Å, 2.155(2) Å, 2.0253(19) Å and 2.201(2) Å) are similar to previously reported values (1.84–2.33 Å) in Zn(II) diclofenac, valproate, indomethacine, ibuprofen, naproxen and sulindac complexes with various nitrogen base ligands.[31,32] N-Zn bond distances (2.128(2) Å and 2.115(2) Å) are also similar to previously reported values i.e. (2.097 Å).[31,32](Table 3)

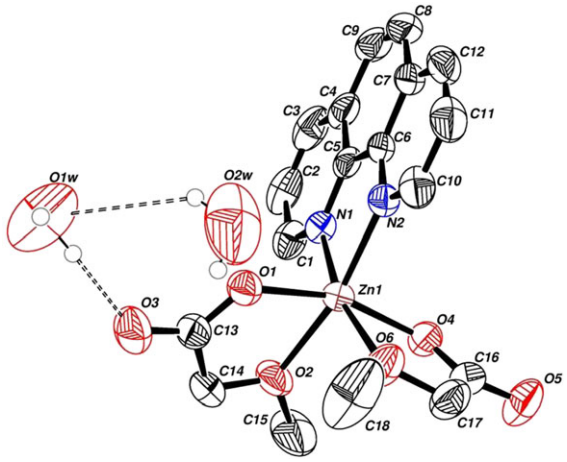

FIGURE 3 Molecular structure of complex **1** showing the labeling atom scheme

Complex **1** adapted slightly distorted octahedral geometry around the central Zn(II) cation due to unsymmetrical bond angles. O(4)-Zn(1)-O(6) = 76.00(8)°, O(2)-Zn(1)-O(6) = 94.62(10)°, O(2)-Zn(1)-O(1) = 76.93(8)°, O(1)-Zn(1)-N(1) = 101.79(8)° and O(4)-Zn(1)-N(2) = 99.33(8)°, N(1)-Zn(1)-N(2) = 79.11(9)°.

Table 2.7 shows the H-bond distances in (Å), these bonds are between O(3), O(4) and O(5) of the methoxyacetate and H of water molecules.(Table 4)

Moreover, in the crystals of complex **1** a π-π interaction with 3.473 Å between the 1,10-phenanthroline ligands are found as shown in Figure 4 which further stabilizes the structure.

3.2.2 | X-ray crystal structure of $Zn_2(phenyl)_4(quin)_2$] (2)

The dinuclear with a paddlewheel structure of complex **2** is shown in Figure 5. Two Zn(II) cations are bonded to four bidentate phenylacetate groups in (*syn-syn*) bridging coordination mode and two monodentate quin groups.

The bond distances of O(1)-Zn(1) 2.060(4) Å, O(2)-Zn(1)#1 2.039(4)Å, O(3)-Zn(1)2.057(4)Å, O(4)-Zn(1)#12.026(4)Å. The coordination distances of N(1)-Zn(1) 2.064(4) Å. Selected bond distances and bond angles are listed in Table 5.

Complex **2** adapted slightly distorted square based pyramidal geometry around the central Zn(II) centers with O(1)-Zn(1)-O(3) = 85.7(2)°, O(1)-Zn(1)-N(1) = 96.35(17)°, N(1)-Zn(1)-O(3) = 97.07(16)°, O(4)#1-Zn(1)-N(1) = 104.37(17)°, O(2)#1-Zn(1)-N(1) = 104.97 (17)°, O(2)#1-Zn(1)-Zn(1)#1 = 80.64(12)° and O(4)#1-Zn(1)-Zn(1)#1 = 80.18(12)°.

3.3 | IR spectroscopy

IR spectroscopy is a functional group technique which plays an important role in structure elucidation. Infrared spectral data of sodium methoxyacetate, complex **1**, sodium phenylacetate, and complex **2** in the 400–4000 cm^{-1} range as KBr pellet are summarized in Tables 6 and 7, respectively.

In metal carboxylate complexes, the major characteristic of the IR spectra is the frequency of the υ asymmetric (υ_{as}) and υ symmetric (υ_s) of carbonyl (COO^-) stretching vibrations and the difference between them $\Delta\upsilon(COO^-)$. The frequency of these bands depends upon the coordination mode of the carboxylate ligand. Monodentate complexes exhibit $\Delta\upsilon(COO^-)$ values that are much greater than those of the ionic carboxylates. Chelating (bidentate) complexes exhibit $\Delta\upsilon(COO^-)$ values that are significantly less than those of the ionic values. $\Delta\upsilon(COO^-)$ values for bridging complexes

TABLE 3 Selected bond angles (°) and bond distances (Å) of **1**

Bond distance (Å)		Bond angle (Å)	
N(1)-Zn(1)	2.128(2)	N(1)-Zn(1)-N(2)	79.11(9)
N(2)-Zn(1)	2.115(2)	O(4)-Zn(1)-N(2)	99.33(8)
O(1)-Zn(1)	2.0269(19)	N(1)-Zn(1)-O(1)	101.79(8)
O(2)-Zn(1)	2.155(2)	O(2)-Zn(1)-O(1)	76.93(8)
O(4)-Zn(1)	2.0253(19)	O(2)-Zn(1)-O(6)	94.62(10)
O(6) -Zn(1)	2.201(2)	O(4)-Zn(1)-O(6)	76.00(8)
C(1)-N(1)	1.328(4)	C(1)-N(1)-C(5)	118.5(2)
C(5)-N(1)	1.355(3)	C(1)-N(1)-Zn(1)	129.1(2)
C(6)-N(2)	1.347(4)	C(5)-N(1)-Zn(1)	112.34(17)
C(10)-N(2)	1.334(4)	C(6)-N(2)-C(10)	118.4(2)
C(13)-O(1)	1.269(4)	C(10)-N(2)-Zn(1)	128.7(2)
C(14)-O(2)	1.416(4)	C(6)-N(1)-Zn(1)	112.89(18)
C(15)-O(2)	1.422(4)	Zn(1)-O(1)-C(13)	120.22(19)
C(16)-O(4)	1.265(4)	C(14)-O(2)-Zn(1)	114.54(17)
C(17)-O(6)	1.418(4)	C(15)-O(2)-Zn(1)	130.0(2)
C(18)-O(6)	1.403(4)	C(14)-O(2)-C(15)	113.8(3)
		Zn(1)-O(4)-C(16)	121.84(19)
		Zn(1)-O(6)-C(17)	113.77(18)
		Zn(1)-O(6)-C(18)	130.8(2)
		C(17)-O(6)-C(18)	114.3(3)

TABLE 4 Hydrogen bonds in complex **1** [Å and °]

D-H...A	d(D-H)	d(H...A)	d(D...A)	<(DHA)
O(2 W)-H(2 W2)...O(5)#1	0.87	2.62	3.035(6)	110.8
O(1 W)-H(2 W1)...O(4)#1	0.93	2.02	2.914(4)	161.2
O(1 W)-H(1 W1)...O(3)	0.90	2.00	2.900(5)	173.1

Symmetry transformations used to generate equivalent atoms: #1 x, y + 1, z

are greater than those of chelating complexes, and close to the values of the ionic carboxylates.[33]

The stretching vibrations for sodium phenylacetate υ_{as} (COO^-) and $\upsilon_s(COO^-)$ have been observed at 1562.2 cm^{-1} and 1387.1 cm^{-1}, respectively, and ($\Delta\upsilon COO^-$) is 175.1 cm^{-1}. For sodium methoxyacetate $\upsilon_{as}(COO^-)$ and $\upsilon_s(COO^-)$ are observed at 1610.9 cm^{-1} and 1427.4 cm^{-1}, respectively and ($\Delta\upsilon COO^-$) is 183.5 cm^{-1}.

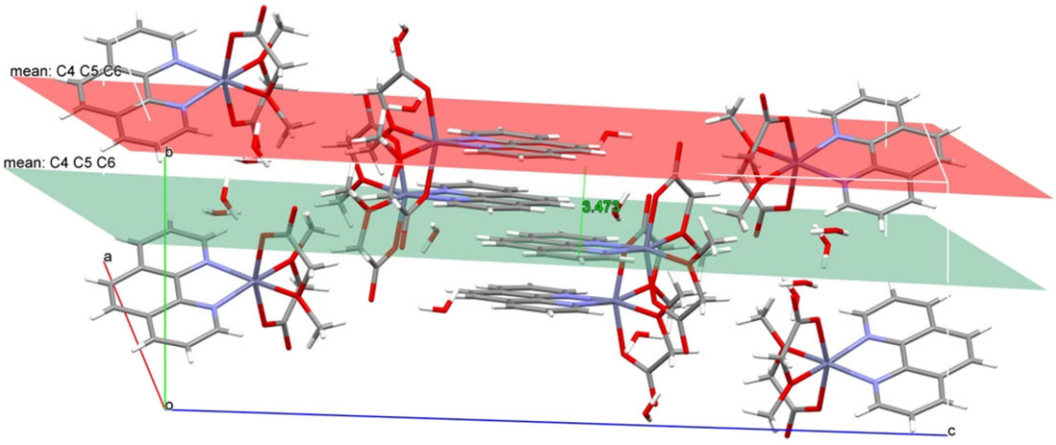

FIGURE 4 π-π interaction between the 1,10-phenanthroline ligands in complex **1**

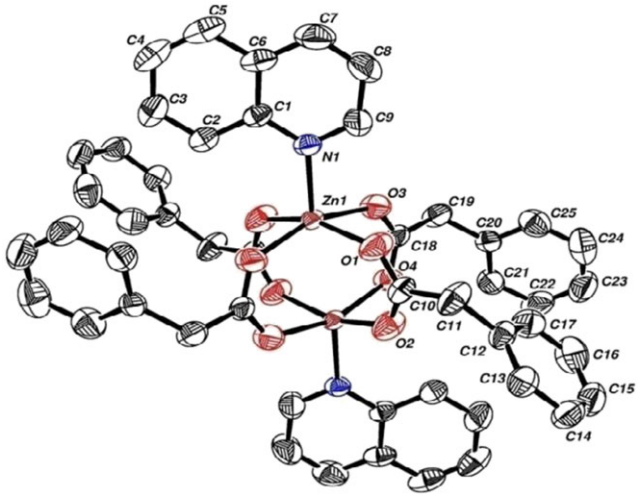

FIGURE 5 Molecular structure of complex **2** showing the labeling atom scheme

In complex **1**; $\upsilon_{as}(COO^{-})$ and $\upsilon_{s}(COO^{-})$ are observed at 1597.1 cm^{-1} and 1425.9 cm^{-1}, respectively, with $\Delta\upsilon COO^{-}$ at 171.2 cm^{-1}, which is less than that of sodium methoxyacetate, this is supporting a bidentate (chelating) coordination mode. The O-H vibration frequency at 3440 cm^{-1} indicates the presence of water molecules in the crystal structure. Generally, the ν(M-O) and ν(M-N) for metal complexes appear as weak bands in the ranges between 430–474 cm^{-1} and 524–576 cm^{-1}.[34] These bands for complexes **1** and **2** are shown in Tables 6 and 7 respectively.

In complex **2**; $\Delta\upsilon COO^{-}$ is 132.3 cm^{-1}, which is less than that of sodium phenylacetate, this is supporting a bidentate (*syn-syn* bridging) coordination mode.

3.4 | ^{1}H and ^{13}C nuclear magnetic resonance

The ^{1}H and ^{13}C NMR spectral data of complex **1,** Zn-methoxyacetate and methoxyacetic acid[35] are shown in Table 8. The relative intensities of ^{1}H NMR signals are in agreement with the proposed structure. Due to complex formation, change in the resonance chemical shift takes place, where comparison of the ^{1}H NMR spectra of **1** and Zn-methoxy showed a downfield shift in complex **1**, this deshielding effect is caused by the donation of electrons from the carboxylate group to the zinc ion through σ bond. In addition, the O-H resonance in the spectra of complex **1** was absent confirming the coordination with the metal center as shown in Figure 3.

As shown in Tables 8–10 and 11 slight upfield and downfield shifts in methoxyacetic acid and phenylacetic acid were observed due to complexation with Zn metal or/and nitrogen donor ligands.(Figure 6)

3.5 | Electronic absorption spectroscopy

Zn(II) complexes with a spatial configuration of d^{10} and completely filled *d* orbital's have no *d-d* electronic transition bands. From the results shown in Tables 12 and 13, no ligand to metal charge transfer "LMCT" can be observed due to filled *d* orbitals. The bands are assigned to MLCT charge transfer and intra ligand transition e.g. π-π^{*} transition, the spectra of the complexes are similar to those of nitrogen parent ligands with very small blue or red shifts caused by zinc coordination. MLCT bands are

TABLE 5 Selected bond distances (Å) and bond angles (°) of **2**

Bond distance (Å)		Bond angle (°)	
N(1)-Zn(1)	2.064(4)	O(1)-Zn(1)-O(3)	85.7(2)
Zn(1)-Zn(1)#1	2.9773(12)	O(1)-Zn(1)-N(1)	96.35(17)
O(1)-Zn(1)	2.060(4)	N(1)-Zn(1)-O(3)	97.07(16)
O(2)-Zn(1)#1	2.039(4)	O(4)#1-Zn(1)-N(1)	104.37(17)
O(3)-Zn(1)	2.057(4)	O(2)#1-Zn(1)-N(1)	104.97(17)
O(4)-Zn(1)#1	2.026(4)	O(2)#1-Zn(1)-Zn(1)#1	80.64(12)
C(1)-N(1)	1.368(6)	O(1)-Zn(1)-Zn(1)#1	77.81(12)
C(9)-N(1)	1.308(7)	O(3)-Zn(1)-Zn(1)#1	78.25(11)
C(10)-O(1)	1.246(6)	O(4)#1-Zn(1)-Zn(1)#1	80.18(12)
C(18)-O(3)	1.236(6)	C(9)-N(1)-Zn(1)	115.5(4)
		C(1)-N(1)-Zn(1)	126.2(4)
		C(9)-N(1)-C(1)	118.2(5)
		C(10)-O(1)-Zn(1)	129.0(4)
		C(10)-O(2)-Zn(1)#1	126.3(4)
		C(18)-O(3)-Zn(1)	128.7(4)

TABLE 6 Summary of principle peaks in the IR spectra of sodium methoxyacetate and complex **1** in (cm^{-1})

Assignments	Na (methoxy)	Complex 1
ν(O-H)	-	3440
ν(C-H)aliph	2940, 2829	-
$\nu(C\text{-}H)_{ar}$	-	3046, 2995
ν(C-O)	1208, 1110	1101
γ(C-H)	932	849.01
δ(C-H)	1333	1514.22
ν_{as}(COO-)	1610.9	1597.1
νs(COO-)	1427.4	1425.9
$\Delta\nu$(COO-)	183.5	171.2
ν(ring)	-	726.37
ν(ring) + δ(C-H)	-	1342
ν(Zn-O)	-	430

TABLE 7 Summary of principle peaks in the IR spectra of sodium phenylacetate and complex **2** in (cm^{-1})

Assignments	Na-phenyl	Complex 2
$\nu(C\text{-}H)_{ar}$	3025	3027
γ(C-H)	933,710	809
$\nu(C\text{-}H)_{alph}$	2000	2362,1946
ν_{as}(N-H)	-	-
ν_{s}(N-H)	-	-
$\delta(NH_2)$	-	-
(N-H) wagging	-	-
$\nu(C\text{-}NH_2)$	-	-
$\nu(C\text{-}C)_{ring}$	1496	1588
$\nu(C\text{-}C)_{ring}$ + δ(CH)	1281,1186	1316
ν(C-N)	-	1403
ν(Zn-O)	-	483
ν(Zn-N)	-	561

observed around (201–296 nm) with ϵ values around 3000 $Lmol^{-1}$ cm^{-1}.[36,37]

3.6 | BNPP hydrolysis

The ability of metal complexes for phosphate diester hydrolysis is studied in the present work**.** The initial rate of the hydrolysis is determined by measuring the absorption of *p*-nitrophenolate ion at 400 nm and various plots of absorbance versus time were obtained. One of these is shown in Figure 7. The prepared complexes were used as catalysts for the phosphate diester group hydrolysis. The results showed good trend and rates in the BNPP hydrolysis process by complexes **1** and **2**.

The results revealed that the rate of BNPP hydrolysis was better in complex **2** compared to those in complex **1**.

TABLE 8 ^{1}H–NMR spectral data of complex **1**, Zn-methoxyacetate and methoxyacetic acid

Complex 1	Zn-methoxy	H methoxy
-	-	11.00 (OH)
3.50, (s, 3H, CH_3)	3.90 (s, 2H, CH_2)	4.12 (s, 2H, CH_2)
4.03, (s, 2H, CH_2)	3.25 (s, 3H, CH_3)	3.48 (s, 3H, CH_3)
7.83, (m, 2H, CH)		
7.94, (s, 2H, CH)		
8.46, (d, 2H, CH,^{3} $J_{H\text{-}H}$ = 7.8 Hz)		
9.18, (dd, 2H, CH, $^{3}J_{H\text{-}H}$ = 6.3 Hz)		

TABLE 9 ^{13}C NMR spectral data of complex **1,** Zn-methoxyacetate and methoxyacetic acid

^{13}C NMR		
Complex 1	**Zn-methoxy**	**Hmethoxy**
173.84 (C = O)	174.02 (C = O)	174.83 (C = O)
71.21 CH_2	71.44 CH_2	69.33 CH_2
59.01 CH_3	58.25 CH_3	59.35 CH_3
126.79 CH		
124.29 CH		
124.25 CH		
150.01 CH		
149.97 CH		
128.80 CH		

TABLE 10 ^{1}H–NMR spectral data of complex **2**, Zn-phenylacetate and phenylacetic acid

^{1}H NMR		
Complex 2	**Zn-phenyl**	**Hphenyl**
-	-	11.00 (OH)
3.39 (s, 2H, CH_2)	3.39 (s, 2H, CH_2)	3.49 (s, 2H, CH_2)
7.22 (bs, 5H, CH)	7.21 (s, 5H, CH)	7.32 to 7.25 (s, 5H, CH)
7.56 (m, 2H, CH)		
7.75 (m, 1H, CH)		
7.98 (m, 2H, CH)		
8.35 (d, 1H, CH, $^{3}J_{H\text{-}H}$ = 8.1 Hz)		
8.88 (bs, 1H, CH)		

TABLE 11 ^{13}C NMR spectral data of complex **2**, Zn-phenylacetate and phenylacetic acid

Complex 2	Zn-phenyl	Hphenyl
177.64 C = O	176.98 C = O	178.00 C = O
43.99 CH_2	43.11CH_2	41.30 CH_2
151.82 CH	137.91 CH	137.35 CH
138.74 CH	129.69 CH	139.09 CH
137.47 CH	128.31 CH	128.90 CH
130.80 CH	126.21 CH	127.30 CH
129.99 CH		
129.32 CH		
129.10 (CH)		
127.81 (CH)		
126.97 (CH)		
122.68 (CH)		

Moreover, Michaelis–Menten equation was used for calculating the initial rate at different concentrations of BNPP, the results are summarized in Table 14.

One of the suggested mechanisms is shown in Scheme 4: (1) H_2O molecule coordinate with metal complex to produce complex **A**, (2) the oxygen atom on the P = O of the substrate (BNPP) is coordinated to the complex metal ion, forming the intermediate **B**, (3) intramolecular metal hydroxide attacks the positive P atom of BNPP molecule to enhance the release of the *p*-nitrophenol with first order-rate constant (k). This step is considered to be the key step for the hydrolysis, (4) after that H_2O coordinates again with the metal ion quickly, **D** is formed, (5) the intermediate **D** quickly loses *p*-nitrophenol and phosphoric acid, where H_2O is bonded again to the metal(II) ion rapidly, and thus completes the catalytic cycle.[27,38,39]

TABLE 12 UV–visible spectral data for the prepared complexes

Compounds	λ_{max} (nm)	ϵ(Lmol^{-1} cm^{-1})
Zn-phenyl	214	2280.3
	259	202.9
	265	203.68
Zn-methoxy	271	1454.2
	292	565.02
1	271	49119
	292	14563
2	276	5606.4
	287	5359.8

TABLE 13 UV–visible spectral data for pure N-ligands

Ligands	λ_{max} (nm)	ϵ(Lmol^{-1} cm^{-1})
1,10-phen (1*10^{-5} M)	266.0	45919
	225.0	45488
quin (1*10^{-5} M)	204.0	44107
	225.0	41442
	276.0	3605.9

3.7 | Anti-bacterial activity

Before measurement of their biological activity, the solution stability of the complexes was tested and checked periodically by ^1H and ^{13}C NMR in chloroform and DMSO solvents

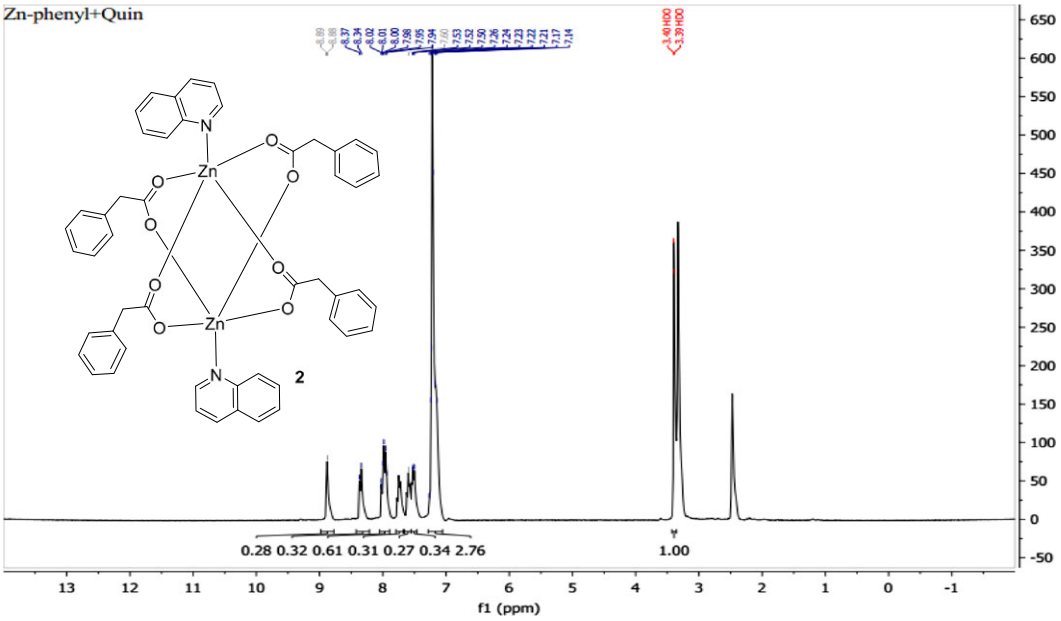

FIGURE 6 ^1H–NMR spectra of complex **2**

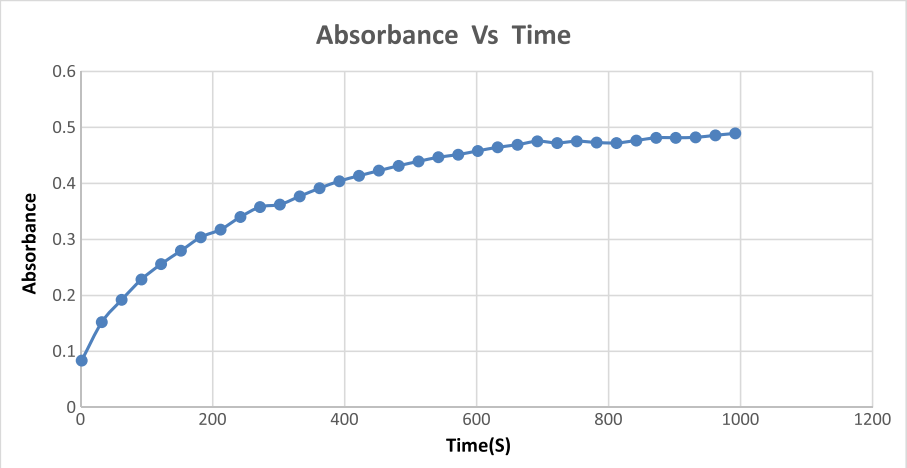

FIGURE 7 BNPP hydrolysis by complex **2** at pH = 7.91, 25°C and [complex] = 1×10^{-4} M

TABLE 14 Kinetic parameters of the BNPP hydrolysis by complexes **1** and **2** at different [BNPP]

Concentration (M)	Initial rate, V_0 mol L^{-1} s^{-1}	Max. Rate, V_{max} mol L^{-1} s^{-1}	Michaelis constant, Km mol L^{-1}	Catalytic rate constant, Kcat[a] s^{-1}	2-order rate constant[b], K[BNPP] L\mol^{-1} s^{-1}
Complex **1**(1×10^{-3} M)					
1×10^{-3}	3.1×10^{-4}	3.16×10^{-4}	6.9×10^{-6}	0.316	4.5×10^{4}
1×10^{-4}	3×10^{-4}				
1×10^{-5}	1.8×10^{-4}				
Complex **2** (1×10^{-4} M)					
1×10^{-3}	9.4×10^{-4}	9.5×10^{-4}	1.5×10^{-5}	9.487	6.2×10^{5}
1×10^{-4}	8.1×10^{-4}				
1×10^{-5}	3.6×10^{-4}				

[a]: $K_{cat} = V_{max}/[complex]$,

[b]: $K_{BNPP} = K_{cat}/K_m$.

and always gave the same data. In addition, the complexes were crystallized by slow solvent evaporation at room temperature that took several days and gave the same physical properties of the compounds. The anti-bacterial activities of the synthesized zinc complexes were studied using different types of gram-negative bacteria (*K. pneumonia*, *E. coli*, *P. Mirabilis* and *P. Aeruginosa*) and gram-positive bacteria (*S. epidermidis*, *S. aureus*, *E. ferabis*, *M. luteus* and *B. Subtilis*) to monitor the effect of complexation on anti-bacteria activity. The average ($n = 3$) IZD inhibition zone diameters with its associated standard error is summarized in Table 15.

$ZnCl_2$, Zn-phenyl and Zn-methoxyacetate did not show any anti-bacterial activity against all tested micro-organisms. DMSO was used as negative control to resist any tested microorganisms, whereas gentamicin (G) and Erythromycin (E) were used as positive control for both G- and G+ bacteria. Complex **2** showed no activity against all tested bacterial species. Complex **1** showed high activity against G- or G+ bacteria except, against *E. ferabis* and *P. Aeruginosa*.

In general, the activity was dependent on the concentration of the complex; this was obvious by the direct proportion found between the concentration and the IZD value. Compounds are considered significantly active when IZD is larger than 15 mm, moderately active when IZD is between 7 and 14 mm and weakly active for IZD less than 7 mm.[40]

Although it is not clear why some compounds exhibit different bacterial activity with Gram-positive and Gram-negative bacteria, it may be ascribed to the difference in the overall structure of their cell walls.[41]

Metal ions are essential for the survival of microbes in the environment or the host. Therefore, the microbes should ensure uptake of metal ions according to their physiological needs as the imbalance in metals homeostasis could be deleterious to the microbe. Host defense against bacterial infection consists of either sequestering ions resulting in bacterial starvation, or increased release of these metals, which results in toxicity. Zinc is required for optimal bacterial growth at a concentration of 10^{-5} to 10^{-7} M,[42] however

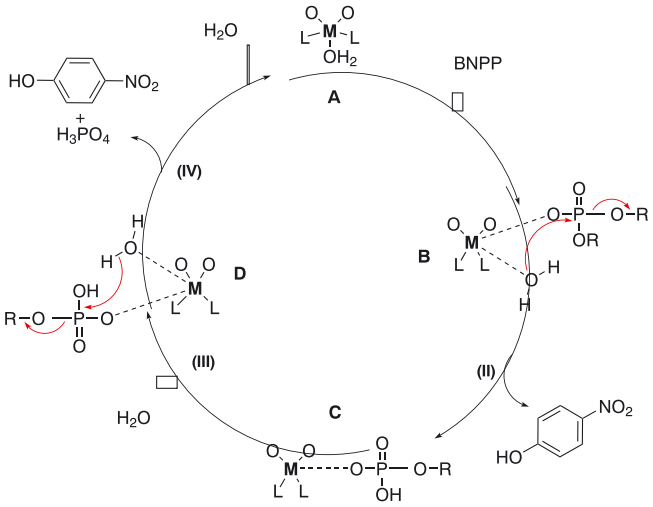

SCHEME 4 The proposed mechanism of the hydrolysis of BNPP

high concentration of zinc ions exhibit antibacterial properties.[43] The toxicity of high concentration of Zn has been shown with infections associated with *Streptococcus pneumonia*,[44] where excess zinc competes with manganese resulting in manganese starvation, and initiation of the oxidative stress in the bacteria, which ultimately leads to bacterial death.[44] It was suggested that zinc exhibit the antibacterial effect by binding to the bacterial membrane, thus increasing the lag phase and the generation time of the organism, which prolongs cell division resulting in cell death.[45] Intriguingly, the zinc oxide (ZnO) nanoparticles have a broad spectrum antibacterial activity against both Gram-negative and Gram-positive bacteria including major foodborne pathogens like *Escherichia coli* O157:H7, *Salmonella*, *Listeria monocytogenes*, *Staphylococcus aureus*, and *Campylobacter jejuni*.[46,47] The antibacterial activity of ZnO has been attributed to the disruption of the cell membrane and the increase in the expression of oxidative stress response genes such as *katA* and *ahpC*) and a general stress response gene (*dnaK*).[47]

Gram-positive bacteria has a plasma membrane and a thick cell wall while the Gram-negative bacteria has plasma membrane, cell wall and an outer membrane which adds another layer of complexity in terms of interaction and penetration of these complexes into the bacteria.

It is not known why complex **2** did not show antibacterial activity against the tested Gram-negative and Gram-positive bacteria. These complexes harbor the zinc ion, the carboxylate group and the nitrogen base. It is plausible that the structural differences in the nitrogen bases of these complexes hindered their binding to the membrane or DNA of the tested bacteria.

The site of action of the non-steroidal anti-inflammatory drugs (NASADs) in human body is determined by inhibiting the synthesis of prostaglandin through effect on cyclooxygenase enzyme.[48] This mechanism is not available in microorganisms due to lack of the presence of cyclooxygenase. Otherwise, killing activity of ibuprofen in *Candida* cells

TABLE 15 Anti-bacterial activity data of complexes **1** and **2**

Compounds	*B. Subtilis* G+	*S. epidermidis* G+	*S. aureus* G+	*E. faecalis* G+	*M. luteus* G+
Zn-phenyl	-	-	-	-	-
Zn-methoxy	-	-	-	-	-
$ZnCl_2$	-	-	-	-	-
DMSO	-	-	-	-	-
G	29.3 ± 4.4	34.7 ± 1.4	29.3 ± 3.2	16.3 ± 0.9	34.7 ± 3.4
E	36.0 ± 2.1	45.0 ± 0.7	41.3 ± 1.4	-	40.0 ± 0.1
1	20.6 ± 1.1	28.7 ± 1.1	27.0 ± 0.8	-	27.6 ± 1.1
2	-	-	-	-	-
Compounds	***K. pneumonia* G-**	***P. Mirabilis* G-**	***E. coli* G-**	***P. Aeruginosa* G-**	
Zn-phenyl	-	-	-	-	
Zn-methoxy	-	-	-	-	
$ZnCl_2$	-	-	-	-	
DMSO	-	-	-	-	
G	34.7 ± 3.4	27.0 ± 1.0	25.3 ± 0.9	20.0 ± 1.8	
E	21.5 ± 0.5	17.3 ± 0.9	24.0 ± 1.6	21.7 ± 3.3	
1	24.3 ± 0.6	25.6 ± 1.4	22.3 ± 1.5	-	
2	-	-	-	-	

was found through direct damage in their cytoplasmic membrane.[49] Intriguingly, it has been shown that Ibuprofen exhibit antibacterial activity against six periodontal microorganisms.[50] The exact mechanism of antibacterial activity of NASIDs is unclear. However, studies have proposed inhibition of bacterial DNA synthesis[51] or impairment of membrane activity.[50]

4 | CONCLUSION

The new Zn(II) complexes with phenylacetic acid and methoxyacetic acid in the presence of the following nitrogen donor ligands; 1,10-phen, quin, were synthesized and characterized. IR, UV–Vis, ^{1}H and $^{13}C\{^{1}H\}$-NMR spectroscopic techniques were used to study and characterize the new complexes. X-ray single crystal diffraction measurements were also studied for complexes **1** and **2** as an additional strong evidence for their structure elucidation. Different metal geometries and carboxylate coordination modes were obtained and proved. The structure of complex **1** revealed slightly distorted octahedral geometry with two bidentate methoxy ligands and one bidentate 1,10-phen ligand bonded to the Zn(II) cations. In complex **2**, slightly distorted square-based pyramidal geometry of the binuclear Zn units was obtained with four phenyl bridging bidentate ligands and two monodentate quin ligands were bonded to the two Zn (II) catinos. The results of the kinetic experiments revealed that these complexes scan act as potent BNPP hydrolysis, these activities were decreased in the order: complex **2** > **1.** Complex **1** exhibited high activity against G- and G+ bacteria except against *E. faecalis* and *P. Aeruginosa*. Complex **2** did not exhibit any activity against G^{-} or G^{+} bacteria.

ACKNOWLEDGEMENT

The authors thank the office of Vice President for Academic Affairs at Birzeit University for their financial support.

REFERENCES

[1] N. S. Krstić, R. S. Nikolić, M. N. Stanković, N. G. Nikolić, D. M. Đorđević, *Trop. J. Pharm. Res.* **2015**, *14*, 337.

[2] N. A. El-Ragehy, M. Abdelkawy, A. El-Bayoumy, *Anal. Lett.* **1994**, *27*, 2127.

[3] S. S. Mitić, G. Z. Miletić, A. N. Pavlović, B. B. Arsić, V. V. Živanović, *J. Serb. Chem. Soc.* **2008**, *73*, 879.

[4] G. A. Lawrance, *Introduction to coordination chemistry*, Vol. 304, John Wiley & Sons Ltd., Chichester **2010**.

[5] C. Dendrinou-Samara, G. Tsotsou, L. V. Ekateriniadou, A. H. Kortsaris, C. P. Raptopoulou, A. Terzis, D. A. Kyriakidis, D. P. Kessissoglou, *J. Inorg. Biochem.* **1998**, *71*, 171.

[6] A. Andrade, S. F. Namora, R. G. Woisky, G. Wiezel, R. Najjar, A. A. Sertiéj, S. D. de Oliveira, *J. Inorg. Biochem.* **2000**, *81*, 23.

[7] N. H. Gokhale, S. S. Padhye, S. B. Padhye, C. E. Anson, A. K. Powell, *Inorg. Chim. Acta* **2001**, *319*, 90.

[8] Z. Trávníček, M. Maloň, Z. Šindelář, K. Doležal, J. Rolčík, V. Kryštof, M. Strnad, J. Marek, *J. Inorg. Biochem.* **2001**, *84*, 23.

[9] A. T. H. Chaviara, P. C. Christidis, A. Papageorgiou, E. Chrysogelou, D. J. Hadjipavlou-Litina, C. A. Bolos, *J. Inorg. Biochem.* **2005**, *99*, 2102.

[10] N. Jiménez-Garrido, L. Perelló, R. Ortiz, G. Alzuet, M. González-Alvarez, E. Cantón, E. M. Liu-González, S. García-Granda, M. Pérez-Priede, *J. Inorg. Biochem.* **2005**, *99*, 677.

[11] V. Milacic, D. Chen, L. Giovagnini, A. Diez, D. Fregona, Q. P. Dou, *Toxicol Appl Pharm* **2008**, *231*, 24.

[12] A. Pérez-Rebolledo, L. R. Teixeira, A. A. Batista, A. S. Mangrich, A. G. Aguirre, H. Cerecetto, M. González, P. Hernández, A. M. Ferreira, N. L. Speziali, *Eur. J. Med. Chem.* **2008**, *43*, 939.

[13] R. R. Crichton, *Biological Inorganic Chemistry An Introduction*, Elsevier B. V. **2008** 369.

[14] Y. Arafat, S. Ali, S. Shahzadi, M. Shahid, *Bioinorg. Chem. Appl.* **2013**, *2013*.

[15] N. Lipscomb, W. N. Strater, *Chem. Rev.* **1996**, *96*, 2375.

[16] I. Bertini, H. B. Gray, *Bioinorganic Chemistry*, University Science Books, CA **1994**.

[17] M. Oelschlägel, S. R. Kaschabek, J. Zimmerling, M. Schlömann, D. Tischler, *Biotechnol. Reports.* **2015**, *6*, 20.

[18] R. Keshab, Q. Zhang, L. Sen, K. Neil, L. Hua, S. Zeng, W. Guangdi, C. Z. Y. Zhang, *Am. J. Clin. Exp. Urol.* **2014**, *2*, 300.

[19] K. R. Parajuli, Q. Zhang, S. Y. Z. Liu, *Int. J. Mol. Sci.* **2015**, *16*, 3700.

[20] L. W. Karena, A. M. Rebecca, M. U. Lyann, H. Paul, V.-P. Dominik, A. B. S. Sidhu, F. Hisashi, D. R. Paul, A. F. David, *J. Biol. Chem.* **2003**, *278*, 33593.

[21] K. Dong, M. Xiang-Guang, J. D. Ying Liu, K. Xing-Ming, Z. Xian-Cheng, *Physiochem. Eng. Aspects.* **2008**, *324*, 189.

[22] F. Jiang, J. Du, X. Yu, J. Bao, X. Zeng, *J. Colloid Interface Sci.* **2004**, *273*, 497.

[23] J. Florián, A. Warshel, *J. Phys. Chem. B* **1998**, *4*, 719.

[24] L. Jian-zhang, L. Hong-bo, B. Zhou, W. Zeng, S.-y. Qin, J. X. Shen-xin Li, *Transit. Met. Chem.* **2005**, *3*, 278.

[25] SMART-NT V5.6, Bruker AXS GMBH, D-76181 Karlsruhe, Germany, **2002**.

[26] SHELXTL-NT V6.1, BRUKER AXS GMBH, D-76181 Karlsruhe, Germany, **2002**.

[27] J. Li, H. Li, B. Zhou, W. Zeng, S. Qin, S. Li, S. J. Xie, *Transit. Met. Chem.* **2005**, *30*, 278.

[28] http://chemwiki.ucdavis.edu/Core/Physical_Chemistry/Physical_Properties_of_Matter/Atomic_and_Molecular_Properties/Intermolecular_Forces/Specific_Interactions/Hydrogen_Bonding (accessed April 20, 2016).

[29] C. N. Pace, H. Fu, F. K. Lee, J. Landua, S. R. Trevino, D. Schell, R. L. Thurlkill, S. Imura, J. M. Scholtz, K. Gajiwala, J. Sevcik, L.

Urbanikova, J. K. Myers, K. Takano, E. J. Hebert, B. A. Shirley, G. R. Grimsley, *Protein Sci.* **2014**, *23*, 652.

[30] I. Paraschiv, M. Giesbers, B. V. Lagen, F. C. Grozema, R. D. Abellon, L. D. A. Siebbeles, A. T. M. Marcelis, H. Zuilhof, E. J. R. Sudhölter, *Chem. Mater.* **2006**, *18*, 968.

[31] (a) H. Abu Ali, S. N. Omar, M. D. Darawsheh, H. Fares, *J. Coord. Chem.* **2016**, *69*, 1110. (b) H. Abu Ali, H. Fares, M. Darweesh, E. Rappocciolo, M. Akkawi, S. Jaber, *Eur. J. Med. Chem.* **2015**, *89*, 67. (c) H. Abu Ali, B. Jabali, *Polyhedron* **2016**, *107*, 97.

[32] a M. Darawsheh, H. Abu Ali, A. L. Abuhijleh, E. Rappocciolo, M. Akkawi, S. Jaber, S. Maloul, Y. Hussein, *Eur. J. Med. Chem.* **2014**, *82*, 152. (b) H. Abu Ali, S. Maloul, I. Abu Ali, M. Akkawi, S. Jaber, *J. Coord. Chem.* **2016**, *69*, 2514. (c) B. Jabali, H. Abu Ali, *Polyhedron* **2016**, *117*, 249.

[33] H. Kagi, D. Ushijima, R. Iizuka, S. Nakano, T. Nagai, *High Press. Res.* **2008**, *28*, 299.

[34] J. B. Hodgson, G. C. Percy, *Spectrochim. Acta A: Mol. Spectrosc.* **1978**, *34*, 777. Available from: http://sdbs.db.aist.go.jp/sdbs/cgi-bin/direct_frame_top.cgi (accessed March 20, 2016).

[35] S. L. Reddy, T. Endo, G. S. Reddy, *Electronic (Absorption) Spectra of 3d Transition Metal Complexes, Advanced Aspects of Spectroscopy*, (Ed: Dr M. A. Farrukh), InTech **2012**, https://doi.org/10.5772/50128. Available from: http://www.intechopen.com/books/advanced-aspects-of-spectroscopy/electronic-absorption-spectra-of-3d-transition-metal-complexes

[36] A. B. P. Lever, *J. Chem. Educ.* **1974**, *5*, 612.

[37] D. Kou, X-G. Meng, Y. Liu, J. Du, X.-M. Kou, X-C. Zeng, *Colloids Surf. A Physicochem. Eng. Asp.* **2008**, *324*, 189.

[38] W. Jiang, B. Xu, J. Zhong, J. Li, F. Liu, *J. Chem. Sci.* **2008**, *120*, 411.

[39] Z. H. Chohan, C. T. Supuran, *Appl. Organomet. Chem.* **2005**, *19*, 1207.

[40] S. G. K. Atmaca, R. Çicek, *Turk. J. Med. Sci.* **1998**, *28*, 595.

[41] B. Sugarman, *Rev. Infect. Dis.* **1983**, *5*, 137.

[42] T. Söderberg, B. Sunzel, S. Holm, T. Elmros, G. Hallmans, S. Sjöberg, *Scand. J. Plast. Reconstr. Surg. Hand Surg.* **1990**, *24*, 193.

[43] C. McDevitt, A. Ogunniyi, E. Valkov, M. C. Lawrence, B. Kobe, A. G. McEwan, J. C. Paton, *PLoS Pathog.* **2011**, *7*, e1002357.

[44] L. L. Radke, B. L. Hahn, D. K. Wagner, P. G. Sohnle, *Clin. Immunol. Immunopathol.* **1994**, *73*, 344.

[45] N. Jones, B. Ray, K. T. Ranjit, A. C. Manna, *FEMS Microbiol. Lett.* **2008**, *279*, 71.

[46] Y. Xie, Y. He, P. L. Irwin, T. Jin, X. Shi, *Appl. Environ. Microbiol.* **2011**, *77*, 2325.

[47] D. H. Abdelaziz, K. Amr, A. O. Amer, *Int. J. Biochem. Cell Biol.* **2010**, *42*, 789.

[48] C. Pina-Vaz, A. G. Rodrigues, F. Sansonettyet, J. Martinez-De-Oliveira, A. F. Fonseca, P. A. Mårdh, *Infect. Dis. Obstet. Gynecol.* **2000**, *8*, 124.

[49] N. K. Dutta, K. A. Kumar, K. Mazumdar, S. G. Dastidar, *Indian J. Exp. Biol.* **2004**, *42*, 922.

[50] N. K. Dutta, K. Mazumdar, S. G. Dastidar, J. H. Park, *Int. J. Antimicrob. Agents* **2007**, *30*, 242.

SUPPORTING INFORMATION

Additional Supporting Information may be found online in the supporting information tab for this article.

How to cite this article: Abu Ali H, Kamel S, Abu Shamma A. Novel structures of Zn(II) biometal cation with the biologically active substituted acetic acid and nitrogen donor ligands: Synthesis, spectral, phosphate diester catalytic hydrolysis and anti-microbial studies. *Appl Organometal Chem*. 2017:e3829. https://doi.org/10.1002/aoc.3829